Protective effect of sonic hedgehog against oxidized low-density lipoprotein-induced endothelial apoptosis: Involvement of NF-κB and Bcl-2 signaling

HUASHAN HUANG[1,2], HUIZHEN YU[1-3], LIANG LIN[4], JUNMING CHEN[1,2] and PENGLI ZHU[1,2]

[1]Shengli Clinical Medical College of Fujian Medical University; [2]Key Laboratory of Geriatrics, Fujian Provincial Hospital, Fuzhou, Fujian 350001; Departments of [3]Cardiology and [4]Gynecology and Obstetrics, Fujian Provincial Hospital South Branch, Fuzhou, Fujian 350028, P.R. China

Received September 13, 2019; Accepted February 21, 2020

DOI: 10.3892/ijmm.2020.4542

Abstract. Sonic hedgehog (Shh) is pivotally important in embryonic and adult blood vessel development and homeostasis. However, whether Shh is involved in atherosclerosis and plays a role in endothelial apoptosis induced by oxidized low-density lipoprotein (ox-LDL) has not been reported. The present study used recombinant Shh-N protein (rShh-N) and a plasmid encoding the human Shh gene (phShh) to investigate the role of Shh in ox-LDL-mediated human umbilical vein endothelial cell (HUVEC) apoptosis. The present study found that ox-LDL was able to induce apoptosis in HUVECs and that Shh protein expression was downregulated. Furthermore, pretreatment with rShh-N or transfection with phShh increased anti-apoptosis protein Bcl-2 expression and decreased cell apoptosis. These protective effects of rShh-N could be abolished by cyclopamine, which is a hedgehog signaling inhibitor. Furthermore, a co-immunoprecipitation assay was performed to demonstrate that Shh interacted with NF-κB p65 in HUVECs. Additionally, ox-LDL upregulated the phosphorylation of NF-κB p65 and inhibitor of NF-κB-α (IκBα), and these effects decreased notably following rShh-N and phShh treatment. Together, the present findings suggested that Shh serves an important protective role in alleviating ox-LDL-mediated endothelial apoptosis by inhibiting the NF-κB signaling pathway phosphorylation and Bcl-2 mediated mitochondrial signaling.

Correspondence to: Professor Pengli Zhu or Professor Huizhen Yu, Key Laboratory of Geriatrics, Fujian Provincial Hospital, 134 Dongjie Road, Gulou, Fuzhou, Fujian 350001, P.R. China
E-mail: zhupengli7755@163.com
E-mail: yhz200333@126.com

Key words: sonic hedgehog, endothelial apoptosis, oxidized low-density lipoprotein, NF-κB, Bcl-2

Introduction

Atherosclerosis is the basic pathological process of atherosclerotic cardiovascular disease (ASCVD), which remains a common cause of morbidity and mortality globally (1). The vascular endothelium, which is located between the blood and tissues, plays a major role in maintaining body homeostasis. Upon exposure to proatherogenic factors, such as oxidized low-density lipoprotein (ox-LDL), endothelial cells (ECs) undergo a series of changes, including increased permeability, induced inflammation and apoptosis, ultimately disrupting the balance of EC homeostasis and initiating of atherosclerosis (2,3). Apoptosis, a mode of programmed cell death, is a direct consequence of impaired endothelial function. Ox-LDL is associated with an increased risk of endothelial apoptosis and contributes to the pathogenesis of atherosclerosis (4).

Sonic hedgehog (Shh), initially identified in *Drosophila melanogaster*, together with Indian hedgehog and Desert hedgehog, acts as a growth factor, survival agent and inductive signal in a gradient-dependent fashion to determine cell fate (5). This process is pivotally important to blood vessel development and adult homeostasis. The Shh protein undergoes autocatalytic cleavage to produce a mature Shh-N fragment with cholesterol and fatty modifications (6). The canonical Shh signaling pathway begins with the binding of Shh-N to the transmembrane protein Patched (Ptch), relieving the inhibition of Smoothened (Smo), which results in activation of glioma-associated oncogene homolog transcription factors (Gli1, 2 and 3) (7,8).

Hedgehog signaling is critical for maintaining the adult coronary vasculature and an impaired Shh pathway contributes to cardiac dysfunction (9,10). There is growing evidence that hedgehog components, such as Shh and Gli1, are markedly downregulated in the atherosclerotic vasculature (11-13). Exogenous Shh protein has therapeutic potential for repairing oxidative stress-induced endothelial injury by increasing endothelial nitric-oxide synthase (eNOS) expression, inducing nitric oxide release and improving endothelial function (14). Shh signaling pathway activation could reduce astrocyte apoptosis through increasing the expression of the anti-apoptotic protein Bcl-2 (15).

The transcription factor NF-κB is an important regulator of inflammatory responses and apoptosis in atherosclerosis (16). Aberrant NF-κB activation has been regarded as a proatherogenic factor and inhibiting NF-κB signaling has been shown to protect against atherosclerosis (16). Canonical NF-κB activation is controlled by the inhibitor of κB kinase (IKK) complex through phosphorylation. IKK activation phosphorylates inhibitor of NF-κB (IκB), resulting in its degradation and allowing NF-κB to be translocated to the nucleus (17). Upon extracellular stimulation, such as hyperlipidemia or ox-LDL, the activated NF-κB triggers the transcription of target genes, including adhesion molecules, cytokines and apoptosis-associated proteins (18).

Hedgehog pathway components are downregulated in atherosclerosis plaques (12), and aberrant NF-κB signaling pathway activation plays a pivotal role in the development of atherosclerosis (16). A previous study in multiple myeloma demonstrated that hedgehog signaling can regulate the NF-κB signaling pathways via classical and non-classical pathways (19). However, to the best of our knowledge, this relationship is still not clear in atherosclerosis.

The present study investigated the role of Shh and its molecular mechanisms in ox-LDL-induced endothelial apoptosis. Additionally, the present study focused on the effects of Shh on NF-κB pathway phosphorylation. It was found that Shh was downregulated in ox-LDL-induced ECs. Overexpression of Shh demonstrated its protective effect on ox-LDL-mediated cell apoptosis via the NF-κB pathway and Bcl-2 mediated mitochondrial signaling.

Materials and methods

Reagents. Ox-LDL was purchased from Yiyuan Biotechnologies (cat. no. YB-002-1). Recombinant human Shh N-terminus protein (rShh-N) was obtained from Sangon Biotech Co., Ltd. (cat. no. C600310) and dissolved in ddH_2O. Cyclopamine, a hedgehog signaling inhibitor, was purchased from Cayman Chemical Company (cat. no. 11321). Pyrrolidine dithiocarbamate (PDTC) was purchased from Sigma-Aldrich; Merck KGaA (cat. no. P8765). Cell Counting Kit-8 (CCK-8) was purchased from Dojindo Molecular Technologies, Inc. (cat. no. CK04). Antibodies specific for Shh (cat. no. 2207; 1:1,000), cleaved caspase 3 (cat. no. 9662S; 1:500), Bcl-2 (cat. no. 4223; 1:1,000), Bax (cat. no. 2773; 1:1,000), tublin (cat. no. 2148; 1:1,000) and β-actin (cat. no. 4970; 1:1,000), a NF-κB pathway sampler kit including antibodies for IκBα, phosphorylated (p)-IκBα, p-IKKα/β, NF-κB p65 and p-NF-κB p65 (cat. no. 9936; all used at 1:1,000) and horseradish peroxidase-conjugated goat anti-rabbit IgG (cat. no. 7074; 1:1,000) and horseradish peroxidase-conjugated goat anti-mouse IgG (cat. no. 7076; 1:1,000) were purchased from Cell Signaling Technology, Inc. Antibodies specific for Smo (cat. no. ab113438; 1:1,000), Ptch (cat. no. ab53715; 1;1,000), Gli1 (cat. no. ab49314; 1:500) and IKKα/β (cat. no. ab178870; 1:1,000) were purchased from Abcam.

Cell culture. HUVECs were obtained from human umbilical cord veins treated with a 0.25% trypsin solution (20). A total of 20 human umbilical cord veins were collected from healthy newborns including 11 males and 9 females, at Fujian Provincial Hospital (Fuzhou, China) between September 2018 and September 2019. The age of the mothers ranged between 25 and 30 years. The research protocol was approved by the Ethics Committee of Fujian Provincial Hospital (approval no. K2018-09-008), informed consent forms were signed by the parents of the newborns, and the procedures were all conducted in compliance with the Declaration of Helsinki. HUVECs were cultured in Endothelial Cell Medium (ScienCell Research Laboratories, Inc.) consisting of basal medium, 5% FBS, 1% EC growth supplement and 1% penicillin/streptomycin solution in a humidified incubator at 37˚C in a 5% CO_2 atmosphere. Cells were used between passages 3 and 5.

Cell viability assay. HUVEC viability was analyzed by CCK-8 assay. A total of $5x10^3$ cells/well were seeded into 96-well plates and incubated for 24 h. To assess the appropriate dose of ox-LDL for further experiments, 10, 20, 50 or 100 μg/ml ox-LDL was added to the cells and incubated at 37˚C for 24 h. In addition, to evaluate the appropriate stimulation time of ox-LDL, 50 μg/ml ox-LDL was added to the cells and incubated at 37˚Cfor 4, 8, 12, 24 and 48 h. The absorbance at a wavelength of 450 nm was measured after CCK-8 solution was added to the wells for 2 h.

Western blotting. HUVECs were incubated with 10, 20, 50 or 100 μg/ml ox-LDL for 24 h at 37˚C or 1, 10 and 100 ng/ml rShh-N for 24 h at 37˚C. Alternatively HUVECs were treated with 20 μM cyclopamine for 2 h at 37˚C or 20 μM PDTC for 1 h at 37˚C. Subsequently, total protein was extracted with RIPA lysis buffer (cat. no. P0013C; Beyotime Institute of Biotechnology) added protease/phosphatase inhibitor cocktail (cat. no. 5872; Cell Signaling Technology, Inc.) on ice for 30 min. The samples were then centrifuged at 12,000 x g for 15 min at 4˚C, and protein quantification was performed using BCA protein assay kit (cat. no. 23227; Thermo Fisher Scientific, Inc.), according to the manufacturer's protocol. Following heat treatment at 99˚C, 50 μg protein samples from the different groups were separated by 8-12% SDS-PAGE and transferred to PVDF membranes. Blocking was performed with 5% bovine serum albumin (cat. no. 9998; Cell Signaling Technology, Inc.) for 2 h at room temperature. Primary antibodies specific for Shh, Smo, Ptch, Gli1, cleaved caspase 3, Bcl-2, Bax, IκBα, p-IκBα, IKKα/β, p-IKKα/β, NF-κB p65, p-NF-κB p65, Tublin and β-actin were incubated with the membranes overnight at 4˚C. The next day, secondary antibodies specific for horseradish peroxidase-conjugated goat anti-rabbit IgG and horseradish peroxidase-conjugated goat anti-mouse IgG were incubated with the membranes at room temperature for 1 h and the proteins were visualized using the WesternBright enhanced chemiluminescence (cat. no. K-12045-D50; Advansta, Inc.). Image J (version 1.4; National Institutes of Health) was used to quantify the western blots.

Plasmid transfection. Commercialized plasmid encoding the human Shh gene (phShh) and pFlag were synthesized by General Biosystems Co., Ltd. The control plasmid, pFlag, constructed by inserting Flag tag sequence 5'-GATTACAAGGATGACGACGATAAG-3' into the plasmid pcDNA3.1/Hygro(+). phShh was constructed by inserting

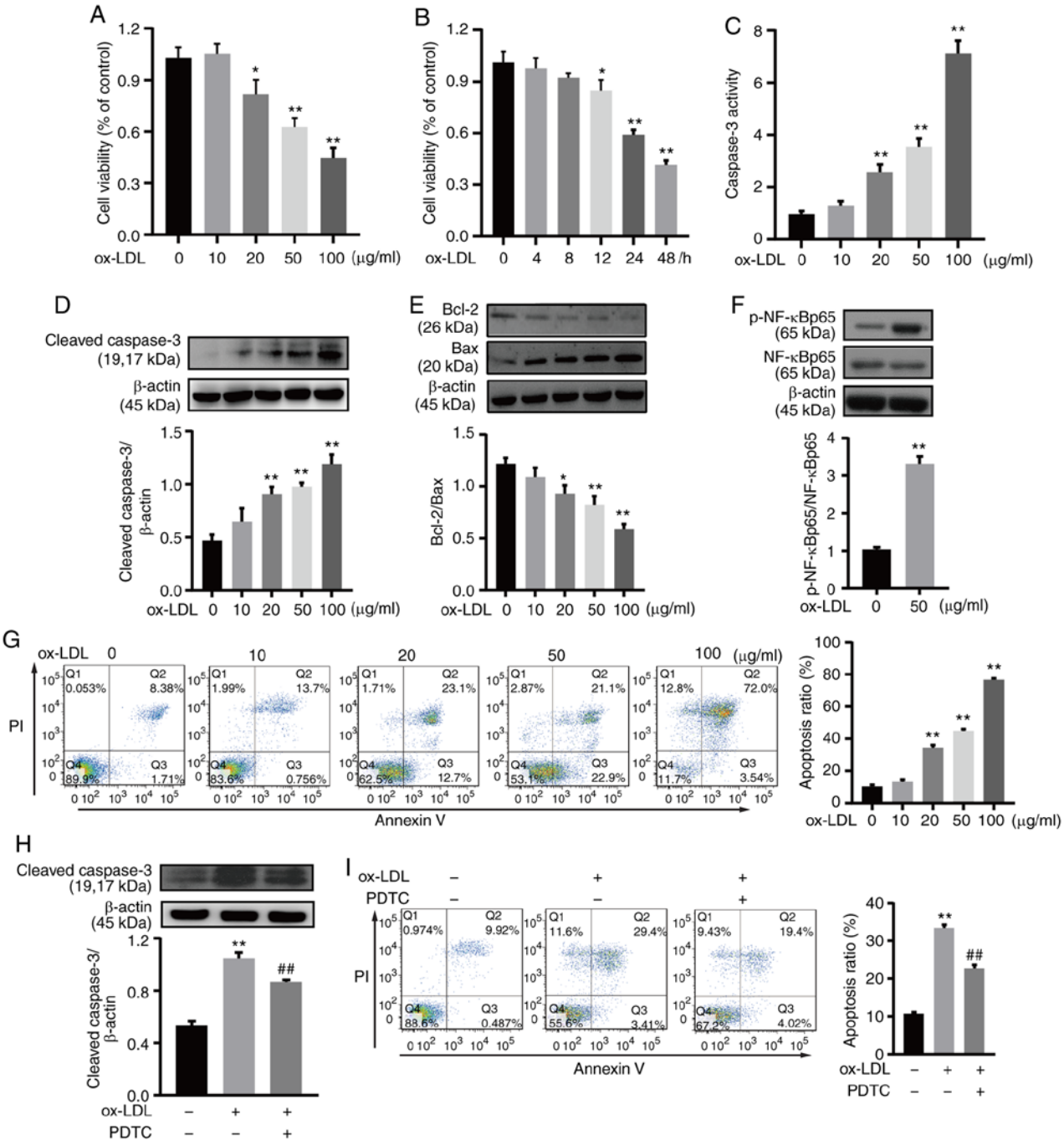

Figure 1. Ox-LDL induced HUVEC apoptosis and the phosphorylation of NF-κB. (A) HUVECs were exposed to ox-LDL for 24 h. Cell viability was gradually downregulated in a dose-dependent manner. (B) HUVECs exposed to 50 μg/ml ox-LDL for 4-48 h, exhibited a progressive decrease in cell viability in a time-dependent manner. (C) HUVECs were treated with ox-LDL for 24 h, and caspase 3 activity was determined at A405 nm using a caspase 3 activity assay kit. (D) HUVECs were treated with 50 μg/ml ox-LDL for 24 h, then cell lysates were prepared and subjected to western blot analysis for the detection of cleaved caspase 3 expression. β-actin was used as an internal loading control. (E) HUVECs were treated with 50 μg/ml ox-LDL for 24 h, then western blot analysis was performed to detect Bcl-2 and Bax expression, and the Bcl-2/Bax ratio was calculated. (F) HUVECs were treated with 50 μg/ml ox-LDL for 60 min, then western blot analysis was used to detect p-NF-κB p65 and NF-κB p65 expression. β-actin was used as an internal loading control. (G) HUVECs were treated with ox-LDL for 24 h, and apoptosis was analyzed by Annexin V/PI staining. Q1, dead cells; Q2, late apoptotic cells; Q3, early apoptotic cells; and Q4, viable cells. Apoptotic cells were considered as Q2 and Q3. (H) HUVECs were treated with 20 μM PDTC and 50 μg/ml ox-LDL, followed by western blot analysis for the detection of cleaved caspase 3 expression. β-actin was used as an internal loading control. (I) HUVECs were treated with 20 μM PDTC and 50 μg/ml ox-LDL, and apoptosis was analyzed by Annexin V/PI staining. Q1, dead cells; Q2, late apoptotic cells; Q3, early apoptotic cells; and Q4, viable cells. Apoptotic cells were considered as Q2 and Q3. All experiments were repeated three times and the data are presented as the mean ± standard deviation. *P<0.05, **P<0.01 vs. untreated control. $^{\#\#}$P<0.01 vs. ox-LDL only-treated group. PDTC, pyrrolidine dithiocarbamate; ox-LDL, oxidized low-density lipoprotein; HUVEC, human umbilical vein endothelial cell; p-, phosphorylated; PI, propidium iodide.

a 1,425 bp Shh gene fused with Flag tag sequence into the plasmid pcDNA3.1/Hygro(+). HUVECs were transfected with 2 μg phShh or pFlag using Lipofectamine® 3000 transfection reagent (cat. no. L3000015; Invitrogen; Thermo Fisher Scientific, Inc.), and then cultured for 48 h before subsequent experiments.

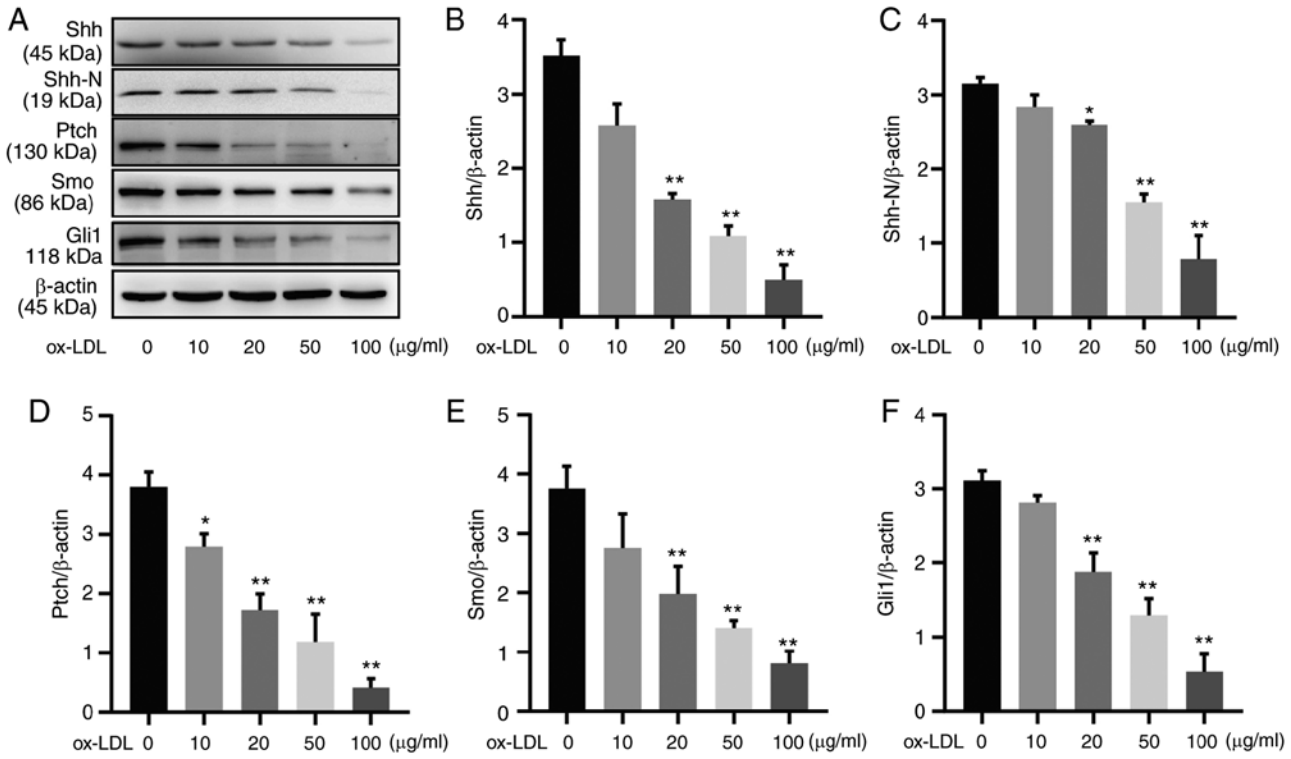

Figure 2. Hedgehog signaling is downregulated in ox-LDL induced HUVECs. (A) HUVECs were treated with ox-LDL for 24 h, and western blot analysis of hedgehog signaling components was performed. Quantification of (B) Shh, (C) Shh-N, (D) Ptch, (E) Smo and (F) Gli1 protein expression. All experiments were repeated three times and the data are presented as the mean ± standard deviation. *P<0.05, **P<0.01 vs. untreated control group. ox-LDL, oxidized low-density lipoprotein; HUVEC, human umbilical vein endothelial cell; Shh, Sonic hedgehog; Shh-N, Sonic hedgehog N-terminus; Ptch, patched; Smo, smoothened; Gli1, glioma-associated oncogene homolog 1.

Co-immunoprecipitation (Co-IP) assay. HUVECs were lysed with cell lysis buffer for western and IP (cat. no. P0013; Beyotime Institute of Biotechnology) and centrifuged at 12,000 x g for 15 min at 4˚C. The protein lysates were incubated with protein A/G plus agarose beads (cat. no. sc-2003; Santa Cruz Biotechnology, Inc.) and antibodies specific for Shh (1:100) or NF-κB p65 (1:100) overnight on a rotating device at 4˚C. The normal IgG (cat. no. 2729; Cell Signaling Technology, Inc.; 1:100) was used for the control group. The following day, the immunoprecipitated complexes consisting of antibody, targeted protein and protein A/G plus agarose beads were centrifuged at 1,000 x g for 5 min at 4˚C. Cell lysis buffer for western and IP was used as the washing reagent and the cells were centrifuged at 1,000 x g for 5 min at 4˚C in triplicate. Finally, the complexes were analyzed by western blotting.

Apoptosis analysis by flow cytometry. FITC Annexin V Apoptosis Detection kit was purchased from BD Biosciences (cat. no. 556547) and used for apoptosis detection according to the manufacturer's protocol. Confluent cells were treated under different conditions and then harvested, centrifuged at 1,000 x g for 5 min at room temperature, washed twice with PBS and then resuspended cell in Annexin V Binding Buffer. The cells were stained with 5 μl propidium iodide (PI) and 5 μl Alexa Fluor 488 Annexin V for 15 min at room temperature in the dark. Subsequently, 400 μl Annexin V Binding Buffer was added. Fluorescence was detected using a flow cytometer (FACSVerse; BD Biosciences) and analyzed by BD FACSuite software (Version 1.0; Becton, Dickinson and Company). The unstained cells, cells stained with FITC Annexin V only and cells stained with PI only were used to set up compensation and quadrants.

Caspase 3 activity assay. Caspase 3 activity assay kit (cat. no. C1116; Beyotime Institute of Biotechnology) was used to measure caspase 3 activity according to the manufacturer's protocol. Confluent cells were harvested and lysed using 100 μl lysis buffer on ice for 15 min, then centrifuged at 16,000 x g for 15 min at 4˚C. Subsequently, 50 μl supernatant or lysis buffer (as a control) was mixed with 10 μl Ac-DEVD-pNA and 40 μl detection buffer, followed by incubation at 37˚C for 1 h. The absorbance was detected at 405 nm.

Statistical analysis. All statistical analysis was performed using GraphPad Prism 8.0 (GraphPad Software, Inc.). The data are presented as the mean ± standard deviation (SD), and one-way ANOVA was used to perform statistical comparisons, followed by Tukey's post hoc test. P<0.05 was considered to indicate a statistically significant difference.

Results

Shh expression is downregulated in ox-LDL-induced HUVECs. To investigate the cytotoxicity of ox-LDL in HUVECs, CCK-8 assays were used to examine cell viability. HUVEC viability was decreased by ox-LDL in a dose- and time-dependent manner (Fig. 1A and B). Cell apoptosis was evaluated through the caspase 3 activity, the Bcl-2 and Bax

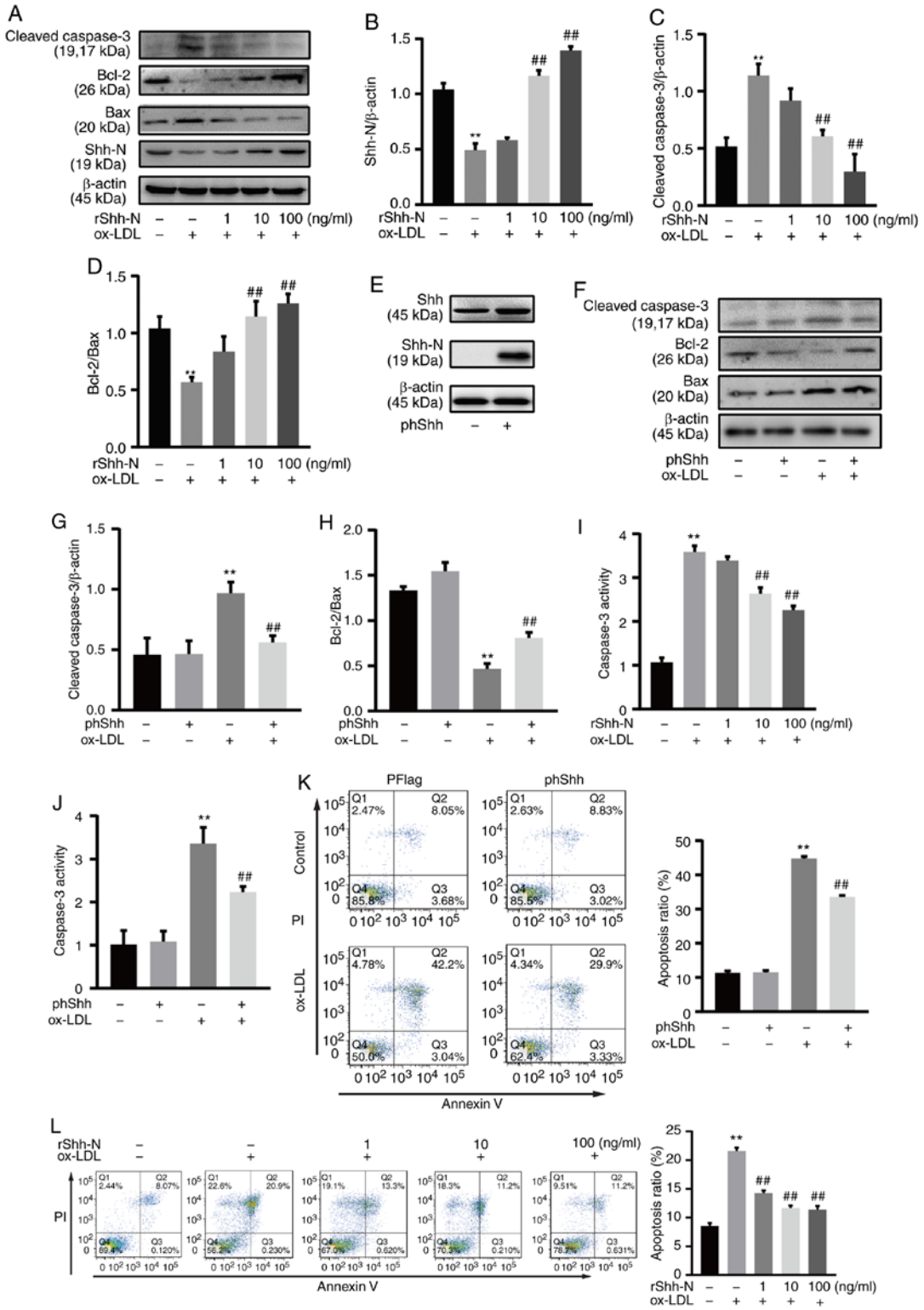

Figure 3. Sonic hedgehog attenuates HUVEC apoptosis. (A) HUVECs were incubated with rShh-N for 24 h and then stimulated with 50 μg/ml ox-LDL for 24 h. Representative western blotting bands of cleaved caspase 3, Bcl-2, Bax and Shh-N are presented. β-actin was used as an internal loading control. Western blot analysis of (B) Shh-N and (C) cleaved caspase 3 relative protein expression and (D) Bcl-2/Bax ratio. (E) HUVECs were transfected with phShh for 48 h, and western blotting demonstrated that the transfection was successful. (F) HUVECs were transfected with phShh for 48 h and then stimulated with 50 μg/ml ox-LDL for 24 h. Representative western blotting bands of cleaved caspase 3, Bcl-2 and Bax are presented. β-actin was used as an internal loading control. Western blot analysis of (G) cleaved caspase 3 relative protein expression and (H) Bcl-2/Bax ratio. (I) HUVECs were incubated with rShh-N for 24 h and then stimulated with 50 μg/ml ox-LDL for 24 h, and caspase 3 activity was determined at A405 nm using a caspase 3 activity assay kit. (J) HUVECs were transfected with phShh for 48 h, and then stimulated with 50 μg/ml ox-LDL for 24 h. Caspase 3 activity was determined at A405 nm using a caspase 3 activity assay kit. (K) HUVECs were transfected with phShh for 48 h, and then stimulated with 50 μg/ml ox-LDL for 24 h, and apoptosis was analyzed by Annexin V/PI staining. Q1, dead cells; Q2, late apoptotic cells; Q3, early apoptotic cells; and Q4m viable cells. Apoptotic cells were considered as Q2 and Q3. (L) HUVECs were incubated with rShh-N for 24 h and then stimulated with 50 μg/ml ox-LDL for 24 h, and apoptosis was analyzed by Annexin V/PI staining. All experiments were repeated three times and the data are presented as the mean ± standard deviation. **P<0.01 vs. untreated control. $^{\#\#}$P<0.01 vs. ox-LDL only-treated group. ox-LDL, oxidized low-density lipoprotein; HUVEC, human umbilical vein endothelial cell; Shh, Sonic hedgehog; Shh-N, Sonic hedgehog N-terminus; rShh-N, recombinant Shh-N protein; phShh, plasmid encoding the human Shh gene; PI, propidium iodide.

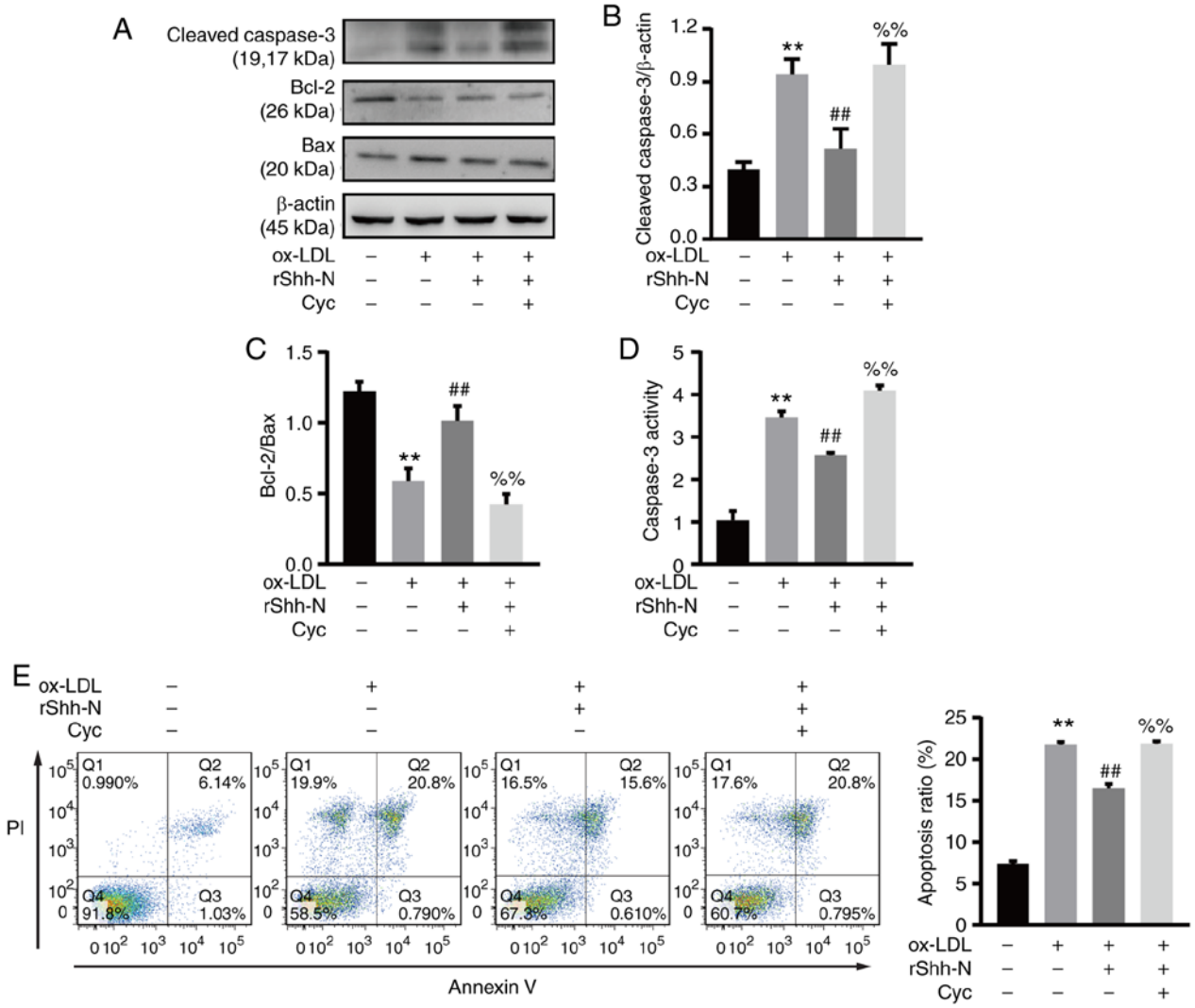

Figure 4. Cyc reverses the effects of Shh-suppressed apoptosis. Human umbilical vein endothelial cells were incubated with 20 μM Cyc for 2 h and then co-cultured with 10 ng/ml rShh-N for 24 h and stimulated with 50 μg/ml ox-LDL for 24 h. (A) Representative western blot bands of cleaved caspase 3, Bcl-2 and Bax. β-actin was used as an internal loading control. Analysis of (B) cleaved caspase 3 relative protein expression and (C) Bcl-2/Bax ratio. (D) Caspase 3 activity was determined at A405 nm by using a caspase 3 activity assay kit. (E) The treated HUVECs were analyzed by Annexin V/PI staining. Q1, dead cells; Q2, late apoptotic cells; Q3, early apoptotic cells; and Q4, viable cells. Apoptotic cells were considered as Q2 and Q3. All experiments were repeated three times and the data are presented as the mean ± standard deviation. **P<0.01 vs. untreated control group. $^{\#\#}$P<0.01 vs. ox-LDL only-treated group. $^{\%\%}$P<0.01 vs. rShh-N and ox-LDL-treated group. Cyc, cyclopamine; Shh, Sonic hedgehog; Shh-N, Sonic hedgehog N-terminus; rShh-N, recombinant Shh-N protein; ox-LDL, oxidized low-density lipoprotein; PI, propidium iodide.

expression, and Annexin V/PI staining. A caspase 3 activity assay kit was used to detect the caspase 3 activity and the results demonstrated that caspase 3 activity was increased by ox-LDL in a dose-dependent manner (Fig. 1C). Consistent with this finding, ox-LDL increased cleaved caspase 3 protein expression in a dose-dependent manner, as indicated by western blotting (Fig. 1D). Additionally, ox-LDL reduced Bcl-2 expression and increased Bax expression, as a consequence, the Bcl-2/Bax ratio was decreased following treatment with ox-LDL. Ox-LDL reduced the Bcl-2/Bax ratio significantly at a dose of 20, 50 or 100 μg/ml (Fig. 1E). Annexin V/PI staining indicated that HUVEC apoptosis increased with increasing ox-LDL concentrations. Following exposure to 25, 50 or 100 μg/ml ox-LDL, the percentage of cells undergoing apoptosis was significantly increased compared with the control group, indicating that apoptosis was the main cause of HUVEC loss (Fig. 1G). Accordingly, 50 μg/ml ox-LDL for 24 h was selected as the appropriate dose and duration for observing ox-LDL-mediated HUVEC apoptosis. Ox-LDL significantly induced the phosphorylation of NF-κB p65 in HUVECs (Fig. 1F). Additionally, the ox-LDL-induced increase in cleaved caspase 3 protein expression was significantly decreased by PDTC, a NF-κB inhibitor (Fig. 1H). Annexin V/PI staining indicated that ox-LDL-induced HUVEC apoptosis was decreased by PDTC (Fig. 1I).

The protein expression of hedgehog signaling family members was evaluated by western blotting in HUVECs treated with 0-100 μg/ml ox-LDL for 24 h (Fig. 2A). HUVECs exposed to 20 μg/ml ox-LDL demonstrated significantly reduced protein expression of both full-length Shh and the Shh-N fragment, which was more notable with 50 or 100 μg/ml ox-LDL stimulation (Fig. 2B and C). These ox-LDL-induced reductions were not limited to Shh; the protein expression

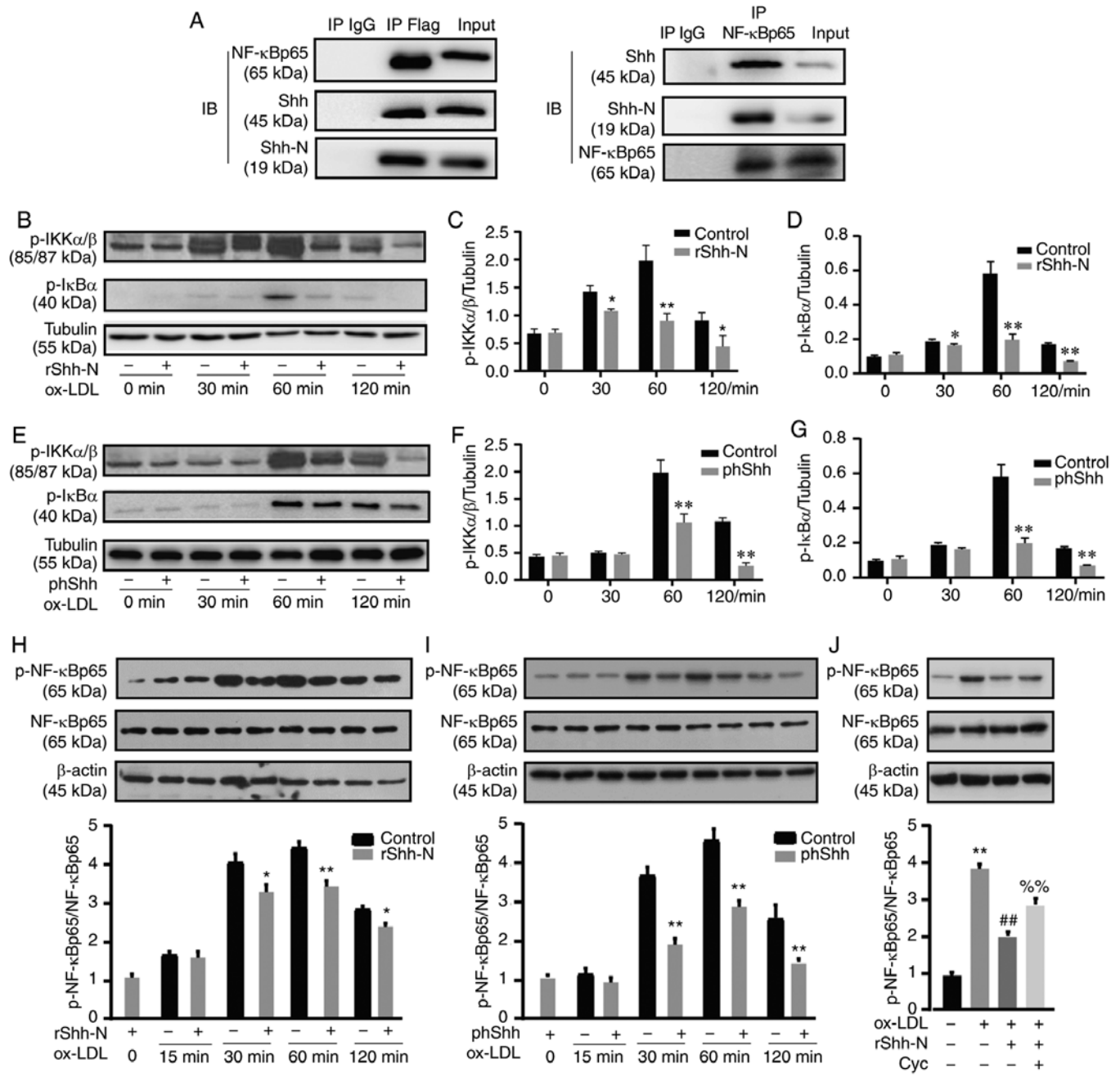

Figure 5. Shh suppresses the phosphorylation of the NF-κB signaling pathway. (A) Co-immunoprecipitation assay was used to reveal the association of Shh and NF-κB p65. (B) HUVECs were co-cultured with 10 ng/ml rShh-N for 24 h and then stimulated with 50 μg/ml ox-LDL for 30-120 min. Representative western blotting bands of p-IKKα/β, total IKKα/β, p-IκBα and total IκBα. Tublin was used as an internal loading control. Relative changes in protein intensity were quantified for (C) p-IKKα/β and (D) p-IκBα. (E) HUVECs were transfected with phShh for 48 h and then stimulated with 50 μg/ml ox-LDL for 30-120 min. Representative western blotting bands of p-IKKα/β, total IKKα/β, p-IκBα and total IκBα. Tublin was used as an internal loading control. Relative changes in protein intensity were quantified for (F) p-IKKα/β and (G) p-IκBα. (H) HUVECs were co-cultured with 10 ng/ml rShh-N for 24 h and then stimulated with 50 μg/ml ox-LDL for 15-120 min. Western blot analysis of p-NF-κB p65 and NF-κB p65 relative protein expression. β-actin was used as an internal loading control. (I) Following transfection with phShh, HUVECs were stimulated with 50 μg/ml ox-LDL for 15-120 min, and western blot analysis of p-NF-κB p65 and NF-κB p65 relative protein expression was performed. β-actin was used as an internal loading control. (J) Cells were incubated with Cyc 20 μM for 2 h and then co-cultured with 10 ng/ml rShh-N for 24 h and stimulated with 50 μg/ml ox-LDL for 60 min. Western blot analysis of p-NF-κB p65 and NF-κB p65 relative protein expression. β-actin was used as an internal loading control All experiments were repeated three times and the data are presented as the mean ± standard deviation. *P<0.05, **P<0.01 vs. control. $^{\#\#}$P<0.01 vs. ox-LDL only-treated group. $^{\%\%}$P<0.01 vs. rShh-N and ox-LDL-treated group. Cyc, cyclopamine; IP, immunoprecipitate; Shh, Sonic hedgehog; Shh-N, Sonic hedgehog N-terminus; rShh-N, recombinant Shh-N protein; ox-LDL, oxidized low-density lipoprotein; p-, phosphorylated; phShh, plasmid encoding the human Shh gene.

levels of Ptch, Smo and Gli1 also decreased in a concentration-dependent manner (Fig. 2D-F). Therefore, ox-LDL treatment reduced the protein expression of Shh signaling components in HUVECs.

Shh attenuates HUVEC apoptosis. To investigate whether Shh plays a role in ox-LDL-induced endothelial apoptosis, rShh-N and phShh were used. rShh-N protein (1, 10 and 100 ng/ml) was added 24 h prior to 50 μg/ml ox-LDL exposure, and Shh-N

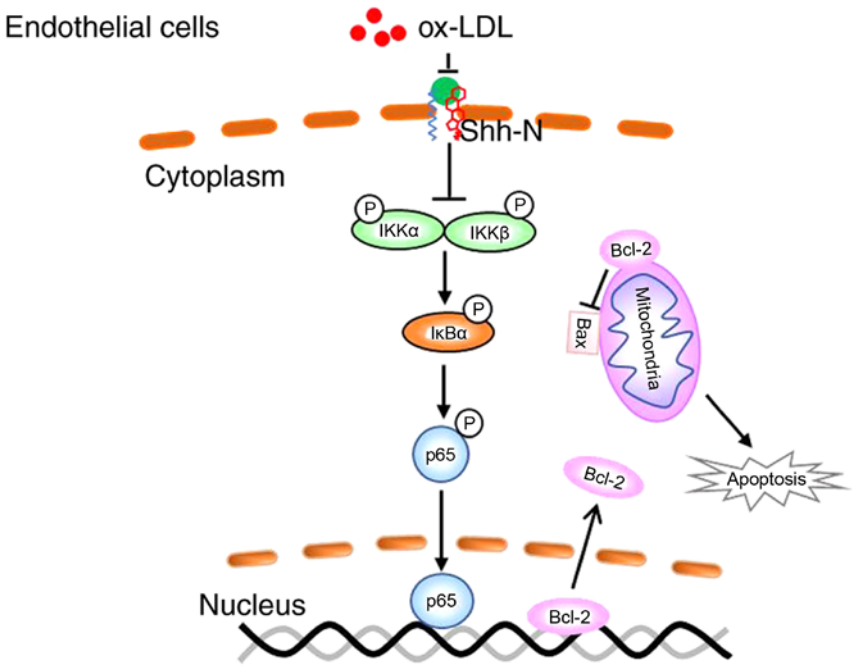

Figure 6. Shh-mediated negative regulation of apoptosis in endothelial cells. Ox-LDL can inhibit Shh-N expression and activate NF-κB by phosphorylating IκB kinase and degrading IκBα. Activated p65 then translocates into the nucleus to promote the expression of apoptosis-related genes. Shh-N functions as a novel NF-κB suppressor by binding to p65 and inhibiting the phosphorylation of IKK, IκBα and p65. Shh, Sonic hedgehog; ox-LDL, oxidized low-density lipoprotein; P, phosphorylated.

expression was significantly enhanced by pretreatment with rShh-N, as determined by western blotting (Fig. 3A and B). Pretreatment with rShh-N significantly decreased cleaved caspase 3 protein expression compared with the group only treated with ox-LDL (Fig. 3C). In addition, rShh-N significantly increased the Bcl-2/Bax ratio compared with cells treated with ox-LDL alone (Fig. 3D). To corroborate this finding, HUVECs were transfected with plasmid encoding either Shh or a control sequence. HUVECs successfully overexpressed Shh and Shh-N following phShh transfection for 48 h, as confirmed by western blotting (Fig. 3E). Consistent with the rShh-N data, following exposure to ox-LDL (50 μg/ml) for 24 h, phShh significantly decreased cleaved caspase 3 protein expression and significantly enhanced the Bcl-2/Bax ratio compared with the control group (Fig. 3F-H). The cells were incubated with rShh-N protein for 24 h or transfected with phShh for 48 h, and then exposed to 50 μg/ml ox-LDL, which demonstrated significant downregulatory effects of rShh-N and phShh on caspase 3 activity compared with the group treated with ox-LDL alone (Fig. 3I and J). The reduction in cell apoptosis was also supported by the Annexin V/PI assay. Following 50-μg/ml ox-LDL stimulation, HUVEC apoptosis was significantly lower in the phShh group compared with the control group (Fig. 3K). The apoptosis rate was significantly increased in the ox-LDL-treated cells pretreated with rShh compared with the cells only treated with ox-LDL (Fig. 3L).

Cyclopamine abolishes the effects of Shh-suppressed endothelial apoptosis. Cyclopamine, a hedgehog signaling inhibitor (21), was used to investigate the effects of Shh-suppressed endothelial apoptosis. The HUVECs were pretreated with 20 μM cyclopamine for 2 h, then treated with 10 ng/ml rShh-N for 24 h and ox-LDL for a further 24 h. Following this treatment, cleaved caspase 3 expression increased and the Bcl-2/Bax ratio decreased significantly compared with the rShh-N and ox-LDL treatment group, suggesting that cyclopamine inhibited the anti-apoptotic effect of rShh-N (Fig. 4A-C). Notably, cyclopamine significantly reversed the Shh-mediated downregulation of caspase 3 activity, and even increased this activity to some extent (Fig. 4D). Finally, Annexin V/PI staining demonstrated that compared with the rShh-N and ox-LDL co-culture group, the percentage of apoptotic cells was increased in the group also pretreated with cyclopamine, indicating that in the presence of cyclopamine, the rShh-N treatment no longer decreases cell apoptosis (Fig. 4E). Thus, cyclopamine abolished the protective effect of the recombinant Shh-N protein.

Shh suppresses NF-κB signaling pathway phosphorylation in ox-LDL-induced HUVECs. To evaluate whether Shh could interact physically with NF-κB p65, a co-IP experiment was performed. Immunoprecipitated Shh from HUVEC lysates produced clear bands for NF-κB p65 and, as expected, immunoprecipitated NF-κB p65 could bind to Shh, revealing that Shh and NF-κB p65 formed a complex (Fig. 5A). Ox-LDL can induce NF-κB activation within 30-60 min (22). To further investigate whether NF-κB signaling was regulated by Shh, the canonical phosphorylation targets in NF-κB signaling were analyzed. Treatment with rShh-N significantly decreased p-IKKα/β and p-IκBα levels during a limited period between 30 and 120 min after ox-LDL treatment (Fig. 5B-D). phShh transfection also significantly decreased p-IKKα/β and p-IκBα levels at 60 and 120 min following ox-LDL treatment (Fig. 5E-G). Specific NF-κB p65 phosphorylation at its ser 536 residue increased progressively and reached a maximum at 60 min. After only 30 min of ox-LDL treatment, rShh-N and phShh

significantly decreased NF-κB p65 phosphorylation compared with the ox-LDL control group (Fig. 5H and I). Cyclopamine significantly reversed the rShh-N-mediated downregulation of NF-κB p65 phosphorylation (Fig. 5J). Together, these findings revealed that Shh exerts its effects on NF-κB signaling by reducing the phosphorylation of p65, IKKα/β and IκBα (Fig. 6).

Discussion

ASCVD is a global health problem that causes death and a substantial economic burden. Perturbation of endothelial integrity initiates atherosclerosis (20). EC apoptosis may result in the loss and turnover of ECs, which contributes to increased vascular permeability, and facilitates the migration and deposition of lipids, further damaging the vasculature and propagating plaque development (23). Additionally, large-scale EC apoptosis results in the denudation of monolayer cells, and exposure of the underlying extracellular matrix can promote thrombosis and increase the risk of plaque disruption (24). The inhibition of EC apoptosis has become a vital target for the prevention and treatment of atherosclerosis (25). The present study demonstrated that activation of the Shh pathway is weakened in ox-LDL-induced HUVECs, that administration of Shh has a protective effect against ox-LDL induced HUVEC apoptosis, and that the protective effect of Shh is mediated by NF-κB p65 pathway in HUVECs.

Previous studies revealed that classical Shh pathway components are obviously decreased in the atherosclerotic vasculature (12) and anti-CD31 antibody labeling of ECs produces Shh immunoreactivity that is not detected in carotid and femoral artery plaques (13). Recently, structural biology studies have focused on the modulated or interaction sites of cholesterol in hedgehog signaling, revealing a direct interaction between cholesterol and Smo, a critical component of the hedgehog signaling cascade, which suggests potential druggable sites (7,26-29). LDL is the main carrier of cholesterol, and ox-LDL plays an important role in atherogenesis (30). The present study used ox-LDL simulation in a hyperlipidemia-induced atherosclerosis in EC, and the results suggested that the expression of Shh, Shh-N, Ptch, Smo and Gli1 were downregulated in a dose-dependent manner, which is consistent with the atherosclerotic vasculature studies *in vivo*.

It has been reported that Shh is pivotally important to vascular remodeling, and induces vascular endothelial growth factor and angiopoietin levels (31). Intramyocardial gene transfer of phShh could preserve left ventricular function by activating hedgehog signaling, and enhanced neovascularization also reduces fibrosis and cardiac apoptosis in acute and chronic myocardial ischemia in adult animals (32). A prior study revealed the protective effect of Shh in astrocytes under oxidative stress and the protective effect of Shh in rat astrocytes under H_2O_2 treatment, which is considered a neuroprotective role against brain injury that is mediated by the PI3K/AKT pathway (33). Compared with previous studies, the present study suggested that NF-κB signaling is critical for the regulation of HUVEC apoptosis by Shh. The effects of the pathway under oxidative stress depends on the different factors, such as cell types, cellular stimuli and environments condition. In addition, Shh could increase eNOS expression and correct angiotensin II-induced hypertension and endothelial dysfunction (34). The present data clearly demonstrate that overexpression of Shh, either by recombinant Shh-N protein or the plasmid encoding the human Shh gene, reduces ox-LDL-induced HUVEC apoptosis by enhancing Bcl-2 expression to regulate mitochondrial apoptosis signaling, and a subsequent downregulation of caspase 3 activity in ox-LDL-treated HUVECs. Furthermore, the anti-apoptotic effect of Shh could be reversed by blocking the Shh signaling pathway with cyclopamin.

Shh undergoes autoproteolysis and yields a mature Shh-N fragment that is modified with N-terminal palmitoyl and C-terminal cholesteryl moieties. Ptch is a 12-transmembrane domain membrane protein and TM2-6 is annotated as its sterol-sensing domain, which is involved in the interaction with Shh-N (35). The classical Shh signaling pathway is initiated by the interaction between Shh-N and Ptch, which relieves the suppression of Smo, subsequently leading to the activation of Gli transcription factor (36). Shh induces angiogenesis in ECs, which does not activate Gli expression or Gli-dependent transcription, but is mediated by the Rho/ROCK pathway (37). Furthermore, several transduction pathways have been reported to be stimulated by Shh. Shh induces angiogenesis in fibroblasts and cardiomyocytes by targeting Notch or Kruppel like factor 2, subsequently activating vascular endothelial growth factor-A expression (38-40). Shh also exhibits an anti-apoptotic effect mediated by the PI3K/AKT/Bcl-2 pathway in astrocytes (33). In addition, Cai *et al* (19) revealed that Shh cross-talks with the NF-κB signaling pathway in multiple myeloma cell lines, and Shh regulates the NF-κB signaling pathway by its classical Smo/Ptch/Gli1 pathway and also by the non-classical Gli1-independent pathway. In the present study, immunoprecipitated Shh from HUVEC lysates revealed the interaction between Shh and NF-κB p65. Shh was able to reduce the phosphorylation of IKKα/β, IκBα and NF-κB p65 stimulated by ox-LDL. Furthermore, the phosphorylation of NF-κB p65 could be reversed by blocking the Shh signaling pathway with cyclopamin. These results confirmed that hedgehog signaling is responsible for decreasing the phosphorylation and activity of NF-κB signaling in ox-LDL-induced HUVECs, which reveals a potential mechanism for improving endothelial apoptosis caused by oxidative stress. The absence of data on whether the enriched proteins could interact with other known binding proteins under ox-LDL treatment is a limitation of the present study.

The morphogen Shh promotes neovascularization in adults (37). In arterial occlusion conditions, blood vessels respond by forming a new capillary network that benefits collateral circulation; however, angiogenesis in atherosclerotic plaques may cause plaque instability, which plays a critical role in the pathogenesis of strokes. Intraplaque neovessels originating from the adventitial vasa vasorum, monocytes or vascular smooth muscle cells may be immature and hence susceptible to rupture (41-43). The mechanisms of angiogenesis in atherosclerosis remain unknown, and its effects on ASCVD remain controversial. However, these effects may be associated with when and where angiogenesis occurs. Agonists and physical or chemical stress can stimulate various cells to generate small membrane-derived vesicles (0.05-1 μm diameter) expressing Shh and the vesicles subsequently shed to neighboring cells, therefore it is reasonable to consider that Shh has a feedback

effect on smooth muscle cells or monocytes; however, the detailed mechanism still requires further investigation (44).

Collectively, the present results are relevant to understanding the association between Shh and pathological atherosclerosis. It was first identified that Shh is a protective protein in ox-LDL-mediated endothelial apoptosis, and that Shh markedly alleviates ox-LDL-induced endothelial apoptosis by blocking the phosphorylation of NF-κB signaling pathway proteins and Bcl-2-controlled mitochondrial signaling.

Acknowledgements

Not applicable.

Funding

This study was supported by the National Natural Science Foundation of China (grant nos. 81873515, 81670258 and 81373785), the Natural Science Foundation of Fujian (grant no. 2017J01247) and the Startup Fund for Scientific Research, Fujian Medical University (grant no. 2017XQ2045).

Availability of data and materials

The datasets used and/or analyzed during the current study are available from the corresponding author on reasonable request.

Authors' contributions

HH designed the study. HH, HY and LL performed the experiments and collected the data. HH, PZ and JC analyzed the data and wrote the manuscript. All authors read and approved the final manuscript.

Ethics approval and consent to participate

The research protocol was approved by the Ethics Committee of Fujian Provincial Hospital (Fuzhou, China; approval no. K2018-09-008), and written informed consent was provided by the parents of the newborns. All procedures were conducted in compliance with the Declaration of Helsinki.

Patient consent for publication

Not applicable.

Competing interests

The authors declare that they have no competing interests.

References

1. Arnett DK, Blumenthal RS, Albert MA, Buroker AB, Goldberger ZD, Hahn EJ, Himmelfarb CD, Khera A, Lloyd-Jones D, McEvoy JW, *et al*: 2019 ACC/AHA Guideline on the primary prevention of cardiovascular disease. A Report of the American College of Cardiology/American Heart Association Task Force on Clinical Practice Guidelines. Circulation 140: e596-e646, 2019.
2. Gimbrone MA Jr and García-Cardeña G: Endothelial cell dysfunction and the pathobiology of atherosclerosis. Circ Res 118: 620-636, 2016.
3. Bar A, Targosz-Korecka M, Suraj J, Proniewski B, Jasztal A, Marczyk B, Sternak M, Przybyło M, Kurpińska A, Walczak M, *et al*: Degradation of glycocalyx and multiple manifestations of endothelial dysfunction coincide in the early phase of endothelial dysfunction before atherosclerotic plaque development in apolipoprotein E/low-density lipoprotein receptor-deficient mice. J Am Heart Assoc 8: e011171, 2019.
4. Ference BA, Ginsberg HN, Graham I, Ray KK, Packard CJ, Bruckert E, Hegele RA, Krauss RM, Raal FJ, Schunkert H, *et al*: Low-density lipoproteins cause atherosclerotic cardiovascular disease. 1. Evidence from genetic, epidemiologic, and clinical studies. A consensus statement from the European Atherosclerosis Society Consensus Panel. Eur Heart J 38: 2459-2472, 2017.
5. Falkenstein KN and Vokes SA: Transcriptional regulation of graded Hedgehog signaling. Semin Cell Dev Biol 33: 73-80, 2014.
6. Qi X, Schmiege P, Coutavas E, Wang J and Li X: Structures of human Patched and its complex with native palmitoylated sonic hedgehog. Nature 560: 128-132, 2018.
7. Huang P, Zheng S, Wierbowski BM, Kim Y, Nedelcu D, Aravena L, Liu J, Kruse AC and Salic A: Structural basis of smoothened activation in hedgehog signaling. Cell 175: 295-297, 2018.
8. Briscoe J and Therond PP: The mechanisms of Hedgehog signalling and its roles in development and disease. Nat Rev Mol Cell Biol 14: 416-429, 2013.
9. Lavine KJ, Kovacs A and Ornitz DM: Hedgehog signaling is critical for maintenance of the adult coronary vasculature in mice. J Clin Invest 118: 2404-2414, 2008.
10. Xiao Q, Hou N, Wang YP, He LS, He YH, Zhang GP, Yi Q, Liu SM, Chen MS and Luo JD: Impaired sonic hedgehog pathway contributes to cardiac dysfunction in type 1 diabetic mice with myocardial infarction. Cardiovasc Res 95: 507-516, 2012.
11. Beckers L, Heeneman S, Wang L, Burkly LC, Rousch MM, Davidson NO, Gijbels MJ, de Winther MP, Daemen MJ and Lutgens E: Disruption of hedgehog signalling in ApoE -/- mice reduces plasma lipid levels, but increases atherosclerosis due to enhanced lipid uptake by macrophages. J Pathol 212: 420-428, 2007.
12. Queiroz KC, Bijlsma MF, Tio RA, Zeebregts CJ, Dunaeva M, Ferreira CV, Fuhler GM, Kuipers EJ, Alves MM, Rezaee F, *et al*: Dichotomy in Hedgehog signaling between human healthy vessel and atherosclerotic plaques. Mol Med 18: 1122-1127, 2012.
13. Dunaeva M, van Oosterhoud C and Waltenberger J: Expression of Hedgehog signaling molecules in human atherosclerotic lesions: An autopsy study. Int J Cardiol 201: 462-464, 2015.
14. Agouni A, Mostefai HA, Porro C, Carusio N, Favre J, Richard V, Henrion D, Martínez MC and Andriantsitohaina R: Sonic hedgehog carried by microparticles corrects endothelial injury through nitric oxide release. FASEB J 21: 2735-2741, 2007.
15. Chen KY, Cheng CJ and Wang LC: Activation of sonic Hedgehog leads to survival enhancement of astrocytes via the GRP78-dependent pathway in mice infected with angiostrongylus cantonensis. Biomed Res Int 2015: 674371, 2015.
16. Yu XH, Zheng XL and Tang CK: Nuclear factor-κB activation as a pathological mechanism of lipid metabolism and atherosclerosis. Adv Clin Chem 70: 1-30, 2015.
17. Maziere C, Auclair M, Djavaheri-Mergny M, Packer L and Maziere JC: Oxidized low density lipoprotein induces activation of the transcription factor NF kappa B in fibroblasts, endothelial and smooth muscle cells. Biochem Mol Biol Int 39: 1201-1207, 1996.
18. Yurdagul A Jr, Sulzmaier FJ, Chen XL, Pattillo CB, Schlaepfer DD and Orr AW: Oxidized LDL induces FAK-dependent RSK signaling to drive NF-κB activation and VCAM-1 expression. J Cell Sci 129: 1580-1591, 2016.
19. Cai K, Na W, Guo M, Xu R, Wang X, Qin Y, Wu Y, Jiang J and Huang H: Targeting the cross-talk between the hedgehog and NF-κB signaling pathways in multiple myeloma. Leuk Lymphoma 60: 772-781, 2019.
20. Lewis LJ, Hoak JC, Maca RD and Fry GL: Replication of human endothelial cells in culture. Science 181: 453-454, 1973.
21. Chen JK: I only have eye for ewe: The discovery of cyclopamine and development of Hedgehog pathway-targeting drugs. Nat Prod Rep 33: 595-601, 2016.
22. Dąbek J, Kułach A and Gąsior Z: Nuclear factor kappa-light-chain-enhancer of activated B cells (NF-κB): A new potential therapeutic target in atherosclerosis? Pharmacol Rep 62: 778-783, 2010.

23. Paone S, Baxter AA, Hulett MD and Poon IKH: Endothelial cell apoptosis and the role of endothelial cell-derived extracellular vesicles in the progression of atherosclerosis. Cell Mol Life Sci 76: 1093-1106, 2019.
24. Luchetti F, Crinelli R, Cesarini E, Canonico B, Guidi L, Zerbinati C, Di Sario G, Zamai L, Magnani M, Papa S and Iuliano L: Endothelial cells, endoplasmic reticulum stress and oxysterols. Redox Biol 13: 581-587, 2017.
25. Choy JC, Granville DJ, Hunt DW and McManus BM: Endothelial cell apoptosis: Biochemical characteristics and potential implications for atherosclerosis. J Mol Cell Cardiol 33: 1673-1690, 2001.
26. Hedger G, Koldsø H, Chavent M, Siebold C, Rohatgi R and Sansom MSP: Cholesterol interaction sites on the transmembrane domain of the hedgehog signal transducer and Class F G protein-coupled receptor smoothened. Structure 27: 549-559.e2, 2019.
27. Weiss LE, Milenkovic L, Yoon J, Stearns T and Moerner WE: Motional dynamics of single Patched1 molecules in cilia are controlled by Hedgehog and cholesterol. Proc Natl Acad Sci USA 116: 5550-5557, 2019.
28. Huang P, Nedelcu D, Watanabe M, Jao C, Kim Y, Liu J and Salic A: Cellular cholesterol directly activates smoothened in hedgehog signaling. Cell 166: 1176-1187.e14, 2016.
29. Zhang Y, Bulkley DP, Xin Y, Roberts KJ, Asarnow DE, Sharma A, Myers BR, Cho W, Cheng Y and Beachy PA: Structural basis for cholesterol transport-like activity of the hedgehog receptor patched. Cell 175: 1352-1364.e1314, 2018.
30. Rajman I, Eacho PI, Chowienczyk PJ and Ritter JM: LDL particle size: An important drug target? Br J Clin Pharmacol 48: 125-133, 1999.
31. Bijlsma MF, Peppelenbosch MP and Spek CA: Hedgehog morphogen in cardiovascular disease. Circulation 114: 1985-1991, 2006.
32. Kusano KF, Pola R, Murayama T, Curry C, Kawamoto A, Iwakura A, Shintani S, Ii M, Asai J, Tkebuchava T, *et al*: Sonic hedgehog myocardial gene therapy: Tissue repair through transient reconstitution of embryonic signaling. Nat Med 11: 1197-1204, 2005.
33. Xia YP, Dai RL, Li YN, Mao L, Xue YM, He QW, Huang M, Huang Y, Mei YW and Hu B: The protective effect of sonic hedgehog is mediated by the phosphoinositide [corrected] 3-kinase/AKT/Bcl-2 pathway in cultured rat astrocytes under oxidative stress. Neuroscience 209: 1-11, 2012.
34. Marrachelli VG, Mastronardi ML, Sarr M, Soleti R, Leonetti D, Martínez MC and Andriantsitohaina R: Sonic hedgehog carried by microparticles corrects angiotensin II-induced hypertension and endothelial dysfunction in mice. PLoS One 8: e72861, 2013.
35. Qi C, Di Minin G, Vercellino I, Wutz A and Korkhov VM: Structural basis of sterol recognition by human hedgehog receptor PTCH1. Sci Adv 5: eaaw6490, 2019.
36. Gong X, Qian H, Cao P, Zhao X, Zhou Q, Lei J and Yan N: Structural basis for the recognition of Sonic Hedgehog by human Patched1. Science 361: eaas8935, 2018.
37. Renault MA, Roncalli J, Tongers J, Thorne T, Klyachko E, Misener S, Volpert OV, Mehta S, Burg A, Luedemann C, *et al*: Sonic hedgehog induces angiogenesis via Rho kinase-dependent signaling in endothelial cells. J Mol Cell Cardiol 49: 490-498, 2010.
38. Chinchilla P, Xiao L, Kazanietz MG and Riobo NA: Hedgehog proteins activate pro-angiogenic responses in endothelial cells through non-canonical signaling pathways. Cell Cycle 9: 570-579, 2010.
39. Caradu C, Couffinhal T, Chapouly C, Guimbal S, Hollier PL, Ducasse E, Bura-Rivière A, Dubois M, Gadeau AP and Renault MA: Restoring endothelial function by targeting desert Hedgehog downstream of Klf2 improves critical limb ischemia in adults. Circ Res 123: 1053-1065, 2018.
40. Morrow D, Cullen JP, Liu W, Guha S, Sweeney C, Birney YA, Collins N, Walls D, Redmond EM and Cahill PA: Sonic Hedgehog induces Notch target gene expression in vascular smooth muscle cells via VEGF-A. Arterioscler Thromb Vasc Biol 29: 1112-1118, 2009.
41. Jaipersad AS, Lip GY, Silverman S and Shantsila E: The role of monocytes in angiogenesis and atherosclerosis. J Am Coll Cardiol 63: 1-11, 2014.
42. Xu J, Lu X and Shi GP: Vasa vasorum in atherosclerosis and clinical significance. Int J Mol Sci 16: 11574-11608, 2015.
43. Zmysłowski A and Szterk A: Current knowledge on the mechanism of atherosclerosis and pro-atherosclerotic properties of oxysterols. Lipids Health Dis 16: 188, 2017.
44. Soleti R and Martínez MC: Microparticles harbouring Sonic Hedgehog: Role in angiogenesis regulation. Cell Adh Migr 3: 293-295, 2009.